Climate Dynamics (2000) 16:369–377

M. R. Van den Broeke

The semiannual oscillation and Antarctic climate, part 5: impact on the annual temperature cycle as derived from NCEP/NCAR re-analysis

Received: 23 August 1999 / Accepted: 28 October 1999

Abstract We use NCEP/NCAR reanalysis data to study the impact of the semiannual oscillation (SAO) on the annual cycle of Antarctic near-surface temperature. When the SAO is weak, the contracted phases (March/April and September/October) are warm and the expanded phases (December/January and June/July) cold. This pattern is explained in terms of the changing meridional fetch of the circumpolar pressure trough. Because of the wave number three character of the SAO, large regional deviations are found. For instance, enhanced north-westerly flow in the second expansion phase (June/July) of weak SAO years limits the growth of the sea ice in the Amundsen and Bellingshausen seas, leading to anomalously high temperatures in the Antarctic Peninsula region. The short (< 50 year) temperature records at Antarctic stations still carry the fingerprint of decadal SAO variability. By matching the observed monthly temperature trends to the patterns derived from the gridded re-analysis, we propose a background Antarctic warming trend for the second expansion phase (June/July) of 4.62 ± 1.02 °C per century, four times the annual value.

1 Introduction

The semiannual oscillation (SAO) is the twice-yearly contraction and expansion of the circumpolar pressure trough (CPT) in middle and high latitudes of the Southern Hemisphere. This happens in response to differences in energy uptake between Antarctica and its oceanic surroundings, forcing a half-yearly wave in baroclinicity, static stability and depression activity (Schwerdtfeger and Prohaska 1956; Van Loon 1967; Meehl 1991; Walland and Simmonds 1999). The SAO is detectable as a significant contribution of the second harmonic to the annual march of surface air pressure, wind speed, cloudiness, precipitation and sea ice cover (Turner et al. 1997; Harangozo 1997; Van den Broeke 2000a, b). Figure 1a shows the location of stations from which observations are used.

The transitions between the four contracted/expanded phases of the SAO represent massive reorganisations of the atmospheric circulation in the Southern Hemisphere. Figure 1b shows the changes in 500 hPa height from March to June in years with a well-developed SAO, and Fig. 1c the concurrent changes in 850 hPa temperature. The northwestward movement of the CPT occurs synchronously with surface pressure rises over the three mid-latitude continents, which strongly amplifies the wave number-3 pattern of the circulation around Antarctica. The associated increase of meridional air exchange causes a reduction of seasonal cooling in regions where the circulation attains a northerly component. Note that the seasonal cooling in New Zealand and the southern parts of South America and Australia are also affected by the SAO: strong cooling occurs in areas where cold Antarctic air is advanced northwards.

Interannual variations in SAO strength represent the dominant mode of Southern Hemisphere circulation variability (Connolley 1997); observation and modelling studies revealed SAO variability on interannual to decadal time scales (Simmonds and Walland 1998). Van den Broeke (1998b) demonstrated that years with a weak/strong SAO are characterised by strong/weak mid-latitude westerlies and limited/enhanced meridional exchange of air between Antarctica and lower latitudes. We use NCEP re-analysis and station data to investigate how this interannual SAO variability impacts on the seasonal cycle of Antarctic temperatures.

M. R. Van den Broeke
Institute for Marine and Atmospheric Research
Utrecht (IMAU) Utrecht University, PO Box 8005,
3508 TA Utrecht, The Netherlands
E-mail: broeke@phys.uu.nl

2 Data and methods

We used monthly averages of surface pressure and 2 m temperature observed at coastal Antarctic stations and monthly means

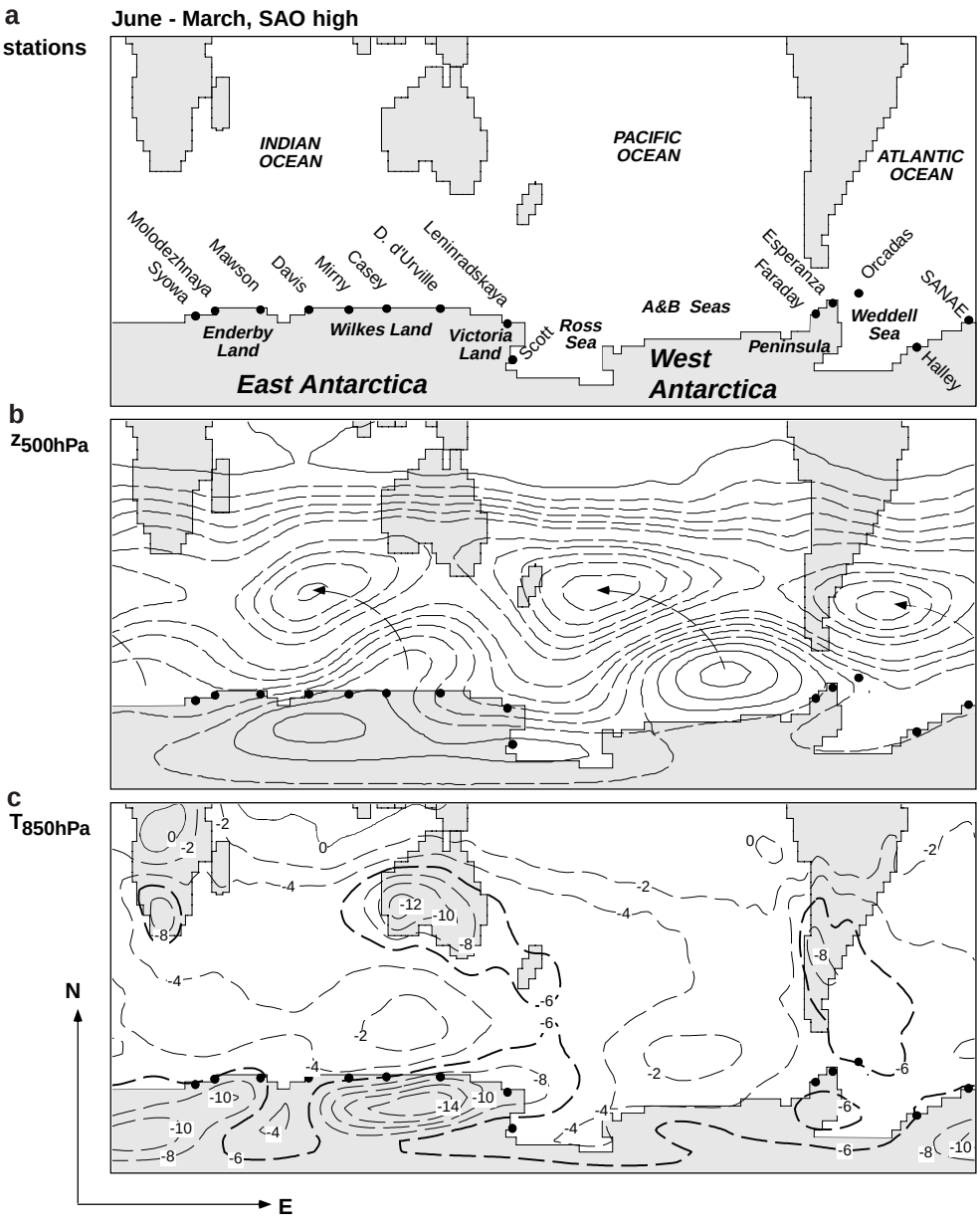

Fig. 1 **a** Location of stations and continental features of the Southern Hemisphere. *A&B* seas: Amundsen/Bellingshausen seas; **b** average change of 500 hpa level height $z_{500\mathrm{hPa}}$ from March to June for 'SAO high' years. Contour interval 10 m, negative values are *dashed*. *Arrows* connect areas of largest changes. **c** Change of 850 hPa temperature $T_{850\mathrm{hPa}}$ from March to June for 'SAO high' years. Contour interval 2 K, negative values are *dashed*. To highlight zonal variations, the −6 K isotherm is printed *bold*

from the NCEP/NCAR re-analysis (NRA) (Kalnay et al. 1996) of 500 hPa height ($z_{500\mathrm{hPa}}$), 850 hPa and 2 m temperatures ($T_{850\mathrm{hpa}}$, $T_{2\mathrm{m}}$) and sea-ice cover on a Gaussian grid with approximately $2° \times 2°$ resolution. Before 1972, NRA uses climatological monthly mean sea-ice cover. It appears that NRA treats the ice shelves as sea ice rather than land ice, an error often found in GCMs (Van den Broeke et al. 1997). This leads to serious overestimation of wintertime surface temperatures. Another problem that negatively affects the reliability of NRA data in the Southern Hemisphere is the erroneous treatment of surface pressure bogus data (PAOBS) for the period 1979–1992. Its degrading impact is large on short time scales, but is small when monthly means are used, as we do here.

To investigate NRA performance in simulating the SAO in Antarctica, Fig. 2 compares the observed and NRA-derived amplitude of the second harmonic in the annual march of surface pressure, $H_2(p)$, at seven representative (sub-) Antarctic stations with reasonably uninterrupted pressure time series. We distinguish between the period before (Fig. 2a) and after 1968 (Fig. 2b). The error is considerably larger before 1968, because in this period NRA does not use Antarctic station data (Bromwich, personal communication 1999); after 1968, NRA performances significantly improves.

We define the strength of the SAO as the zonally and meridionally (40°S–70°S) averaged amplitude of $H_2(p)$, derived from NRA. This quantity is presented in Fig. 3. From the period 1968–97, we selected 11 years that deviate more than one standard deviation (SD) from the mean (thresholds are indicated by solid lines in Fig. 3). These were then stacked to construct 'SAO high' and 'SAO low' fields of the variables under consideration. 1964 was also indicated in the 'SAO-high' stack, because it is well reproduced in the station records. Throughout, results are presented as differences between the mean fields of these two extreme states ('SAO low-high'): $dz_{500\mathrm{hPa}}$, $dT_{850\mathrm{hPa}}$ and $dT_{2\mathrm{m}}$. We furthermore distinguish between four phases in the SAO that represent periods of extreme CPT positions: the expanded phases *Exp. 1* (December/January) and *Exp. 2* (June/July) and the contracted phases, *Con. 1* (March/April) and *Con. 2* (September/October).

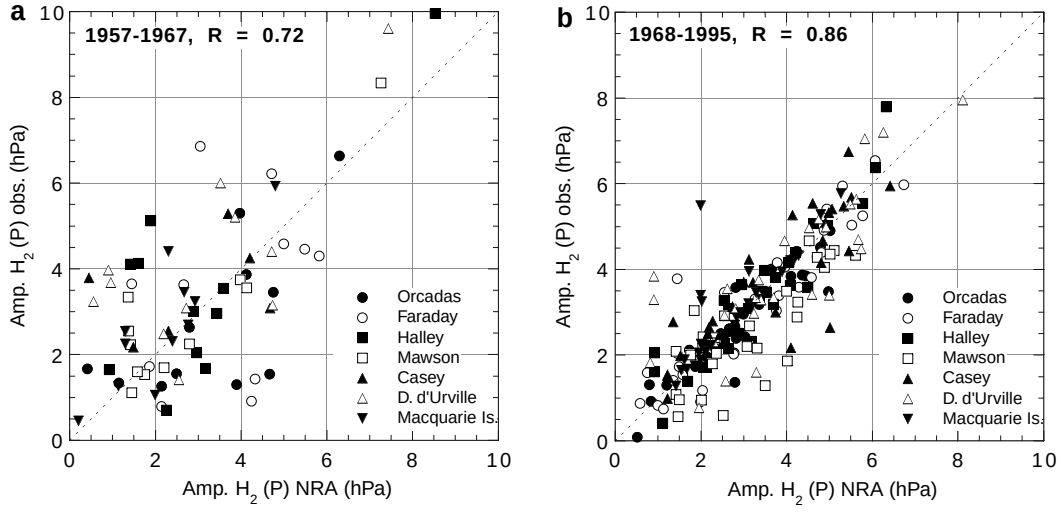

Fig. 2a, b Observed versus NRA-derived values of the amplitude of $H_2(p)$ at seven representative Antarctic stations; **a** 1957–1968 and **b** 1969–1997

3 Anomalies of circulation, temperature and sea ice

3.1 Antarctic averaged anomalies

The upper curves in Fig. 4a, b, c show the annual cycle of $z_{500\text{hPa}}$, $T_{850\text{hPa}}$ and $T_{2\text{m}}$, respectively, averaged over all Antarctic landpoints and over the 6 'SAO-high' years; the lower curves present the 'SAO low-high' anomalies $dz_{500\text{hPa}}$, $dT_{850\text{hPa}}$ and $dT_{2\text{m}}$. A weakly developed SAO translates into a limited meridional amplitude of the CPT movement. As a result, $dz_{500\text{hPa}}$ (Fig. 4a) is negative in the expanded phases, when the CPT fails to move away from the continent, and positive in the contracted phases, when the CPT fails to move towards the continent. Anomalies with opposite signs are found in middle latitudes (not shown). $dT_{850\text{hPa}}$ and $dT_{2\text{m}}$ in Fig. 4b, c are in phase with $dz_{500\text{hPa}}$: weak SAO conditions ensure that in the contracted/expanded phases, the CPT is further north/south than usual, increasing/decreasing the meridional fetch causing positive/negative temperature anomalies over Antarctica (Van den Broeke 1998a). This explains the unexpected observation in coastal East Antarctica that high temperature occur simultaneously with high pressure (Wendler and Kodama 1993). The annual means of $dz_{500\text{hPa}}$, (−16 m), $dT_{850\text{hPa}}$ (−0.16 K) and $dT_{2\text{m}}$ (−0.13 K) are all negative, i.e. changes in the expanded phases dominate. Because changes in the various phases of the SAO tend to cancel, these numbers are not significant. It explains why at individual Antarctic stations no significant correlation is found of the amplitude of $H_2(p)$ with annual mean temperatures.

3.2 Winter anomalies

Because the ice sheet is such a strong heat sink, large vertical and horizontal temperature gradients are constantly present between the continent and its immediate surroundings. Especially in winter, this makes near-surface temperatures very sensitive to changes in the atmospheric circulation. Figure 5 shows the spatial distribution of (a) $dz_{500\text{hPa}}$, (b) $dT_{850\text{hPa}}$ and (c) $dT_{2\text{m}}$ for *Exp. 2* (June/July). The large amplitude of $dz_{500\text{hPa}}$ in *Exp. 2* (Fig. 5a) causes alternating regions of cooling and warming at 850 hPa just north of the Antarctic coastline (Fig. 5b). In the Ross and Amundsen/Bellingshausen Seas we see a decrease of sea-ice cover that is associated with enhanced northerly circulation (advection of warm air) and/or strong westerlies (enhanced mechanical break-up of sea ice). Because the difference in surface temperature between open- and

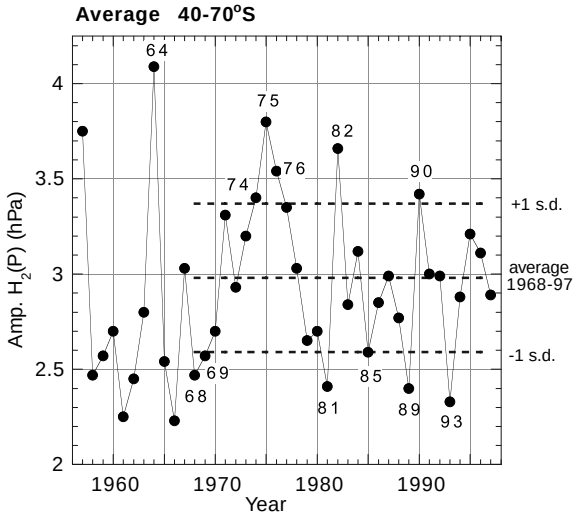

Fig. 3 SAO strength, defined as NRA-derived amplitude of $H_2(p)$, zonally and meridionally (40–70°S) averaged. In the period 1968–1997, 11 individual years are selected for which $H_2(p)$ deviates more than 1σ from the 1968–97 mean

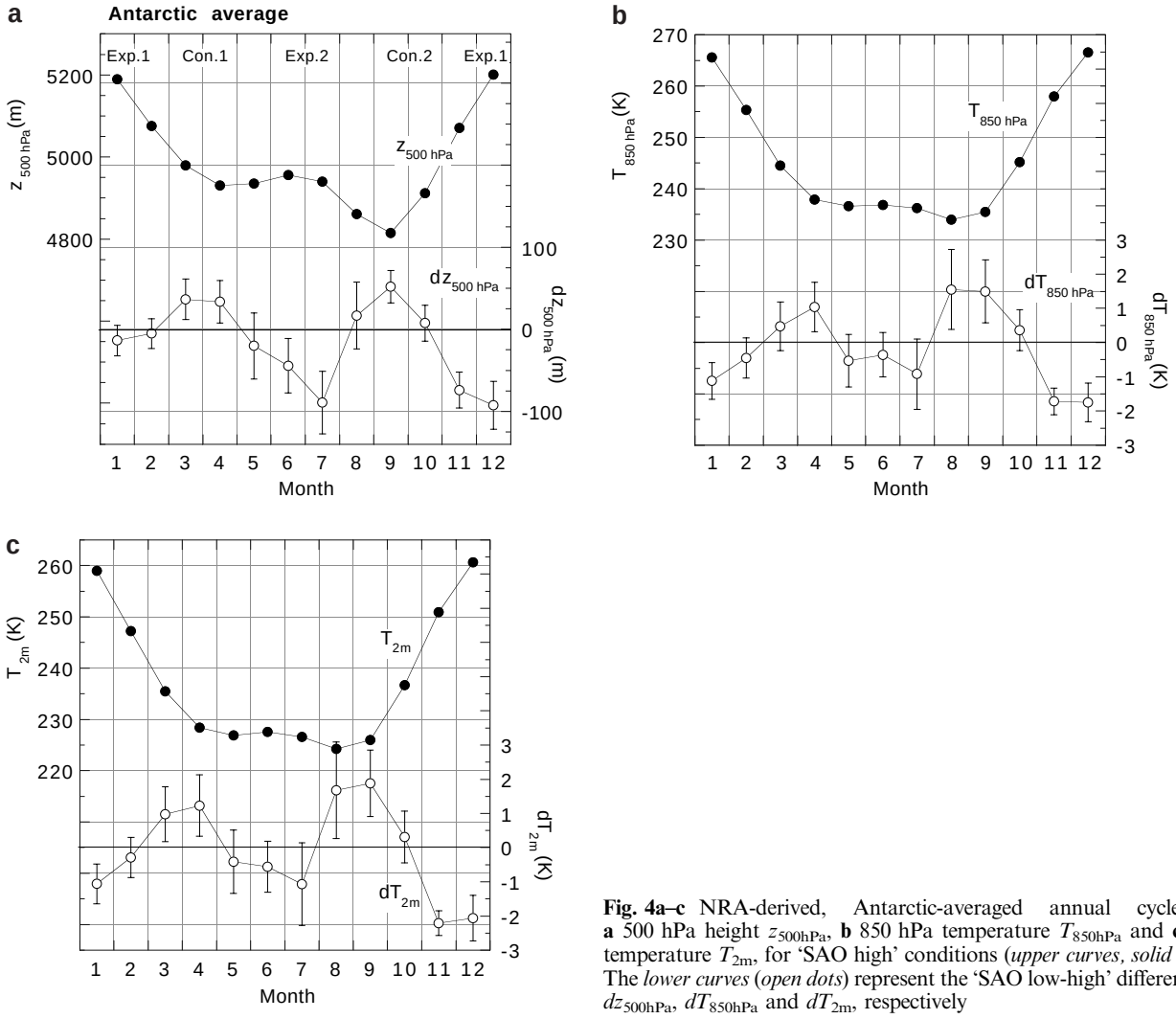

Fig. 4a–c NRA-derived, Antarctic-averaged annual cycle of **a** 500 hPa height $z_{500\mathrm{hPa}}$, **b** 850 hPa temperature $T_{850\mathrm{hPa}}$ and **c** 2 m temperature $T_{2\mathrm{m}}$, for 'SAO high' conditions (*upper curves, solid dots*). The *lower curves* (*open dots*) represent the 'SAO low-high' difference of $dz_{500\mathrm{hPa}}$, $dT_{850\mathrm{hPa}}$ and $dT_{2\mathrm{m}}$, respectively

ice covered water in winter can be as large as 20–30 K, the temperature increase at 2 m is amplified compared to that at 850 hPa in areas where sea-ice cover has decreased (Fig. 5c). This low-level warm air is advected towards the mainland by northerly flow anomalies. Because of its meridional orientation and limited elevation (at least in the model), the impact is especially large on the Antarctic Peninsula (AP), where $dT_{2\mathrm{m}}$ exceeds 6 K on the west coast. The warming that results from the change in sea-ice cover is mostly confined to the atmospheric boundary layer, in agreement with modelling studies that investigate the impact of reduced sea-ice cover on atmospheric temperatures (Van Lipzig 1999). Note that the warm anomalies north of Wilkes Land hardly affect the interior ice cap, a result of the steep ice-sheet topography and the East Antarctic katabatic winds that effectively block upslope transport of the near-surface air.

Because of the seasonal nature of the SAO, circulation anomalies over the AP reverse direction in *Con. 2* (September/October, not shown). With enhanced advection now from the south-east, surface temperature anomalies over the AP are small or even negative, in spite of persistent negative sea-ice anomalies in the Bellingshausen Sea. The large June/July and small September/October warming signal in the AP region is remarkably similar to locally observed temperature trends (King 1994). This is further discussed in Sect. 4.

3.3 A Possible connection between the SAO and formation of the Weddell Polynya?

The positive sea ice anomaly in the eastern Weddell Sea (Fig. 5) is caused by the presence of the Weddell Polynya in three out of six years in the 'SAO-high' stack (1974, 75 and 76). The period of strong SAO that dominates the mid-1970s and the concurrent formation of the Weddell Polynya suggests a connection between the two mechanisms, which could be as follows: as

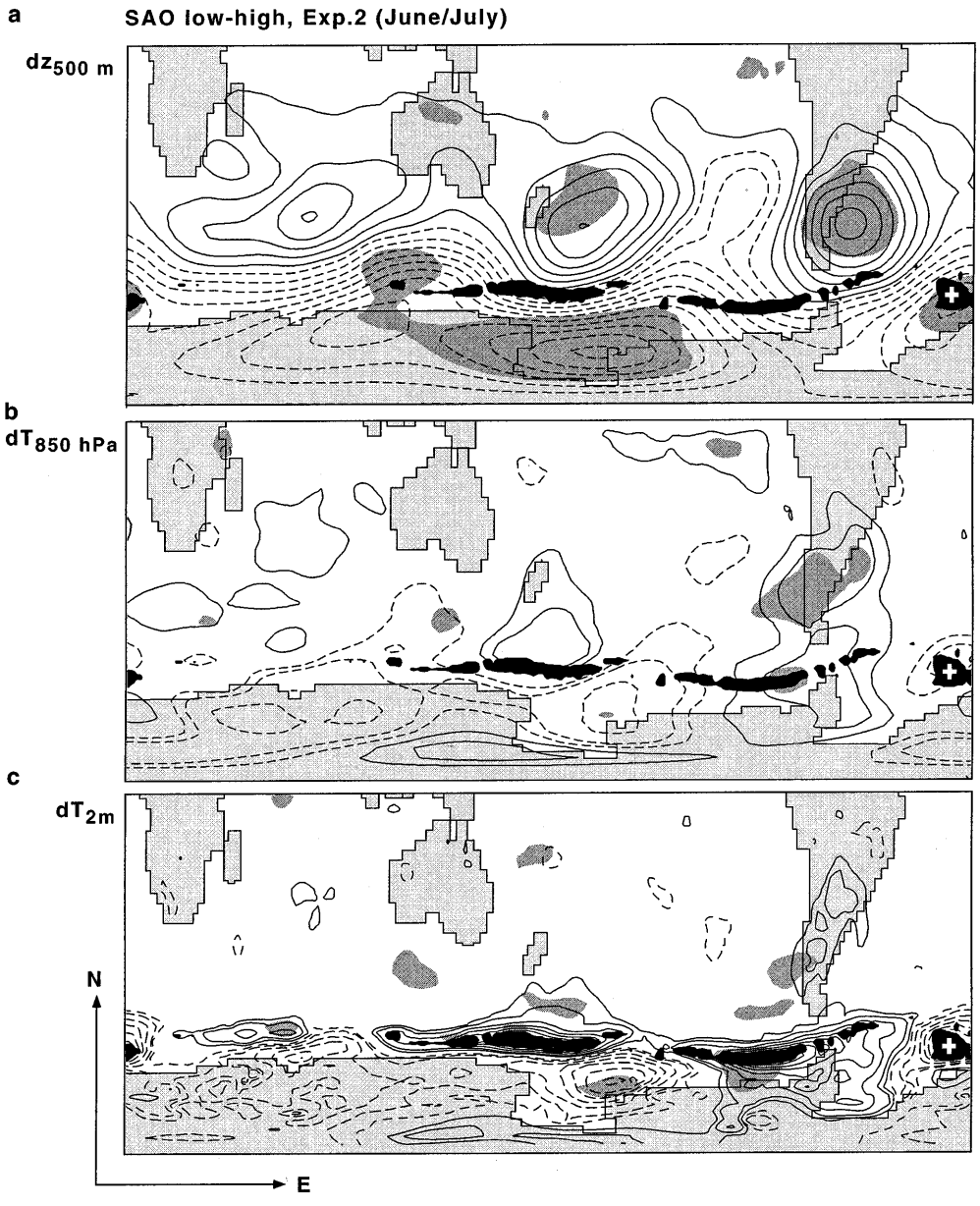

Fig. 5a–c 'SAO low-high' difference fields for expanded phase 2 (June/July) of **a** $dz_{500\text{hPa}}$, **b** $dT_{850\text{hPa}}$ and **c** $dT_{2\text{m}}$. Contour intervals are 10 m for $z_{500\text{hPa}}$ and 1 K for temperature, but the −0.5 and +0.5 K contours are also included. Negative values have *dashed contours*. Areas where confidence level exceeds 95% are *shaded*. *Black areas* denote decrease of sea-ice cover in excess of 15%; the *white* '+' denotes a positive anomaly of the same magnitude

Fig. 1b shows, autumn to winter circulation changes in years with a well-developed SAO cause pronounced advection of lower-latitude air from the north-east towards the eastern Weddell Sea. This results in weak seasonal cooling and divergence of the geostrophic wind (Fig. 1c), which could trigger the formation of the polynya. As Fig. 5a showed, years with a weak SAO are associated with southwesterly flow anomalies in *Exp. 2* (June/July). These transport cold air from the Filchner-Ronne Ice Shelf into the eastern Weddell Sea, a situation that is unfavourable for polynya formation. The polynya was absent in individual years with strong SAO (1982 and 1990, Fig. 3), which could indicate that a prolonged period of strong SAO is required for polynya formation. The link between the SAO and the Weddell Polynya will be explored in a forthcoming paper.

4 SAO variability and temperature trends at Antarctic stations

4.1 Introduction

Antarctic stations exhibits large regional differences in 2 m temperature trends (Jacka and Budd 1998). For example, temperatures at the AP have increased by as much as 2.5 °C over the last 40–50 years (King and Harangozo 1998). This warming is thought to be responsible for the rapid retreat of ice shelves in the region (Vaughan and Doake 1996). On the other hand, the region around Mawson station in East Antarctica has actually cooled. Van den Broeke (1998b) showed that the wave number-3 character of the SAO introduces a longitudinally dependent temperature response

to change in the strength of the SAO. A complicating factor is that local feedbacks modify the temperature response, for instance through the break-up of a strong surface temperature inversion or changes in sea-ice extent (Enomoto and Ohmura 1990). Here we seek evidence that changes in the SAO influenced the annual temperature cycle, by comparing NRA-derived values of dT_{2m} with observed trends of monthly mean temperature at selected Antarctic stations.

4.2 Leningradskaya, Halley and Faraday

Figure 6a–c compares the observed trends of monthly mean temperature (K per century) and NRA-derived values of dT_{2m} at Leningradskaya (1971–1990), Halley and Faraday (1957–1995), respectively. At Leningradskaya there is good agreement between the two: they are in phase both with each other and with the continental mean (compare Fig. 4c). The signal is well preserved at this station, probably because it was operational during a period of significant SAO weakening (1971–1990).

In contrast, observed monthly trends at Halley are exactly out of phase with dT_{2m} (Fig. 6b). The reason is that Halley is situated on the flat Brunt Ice Shelf, some 40 km away from the slope of the inland ice; the station is therefore not influenced by strong katabatic winds, and a, for coastal standards, strong surface inversion of 10–15 K develops in the winter months (King and Turner 1997). This makes near-surface temperatures at Halley very sensitive to changes in cloudiness and near-surface wind speed. Because the SAO-related second harmonics of cloudiness and near-surface wind speed are both in antiphase with the second harmonic of pressure, the temperature response to SAO changes at Halley is opposite to that at other coastal stations (Van den Broeke 2000a). The NRA grid is too coarse to represent the fringing ice shelves and the associated local temperature inversion, which explains the opposite behaviour in Fig. 6b.

The observed annual cycle of warming at Faraday, on the west coast of the AP, has a pronounced wintertime maximum (Fig. 6c). Winter temperatures at Faraday are very sensitive to the extent of sea-ice cover in the Bellingshausen Sea (Jacobs and Comiso 1997) and large-scale circulation patterns (Marshall and King 1998). Van

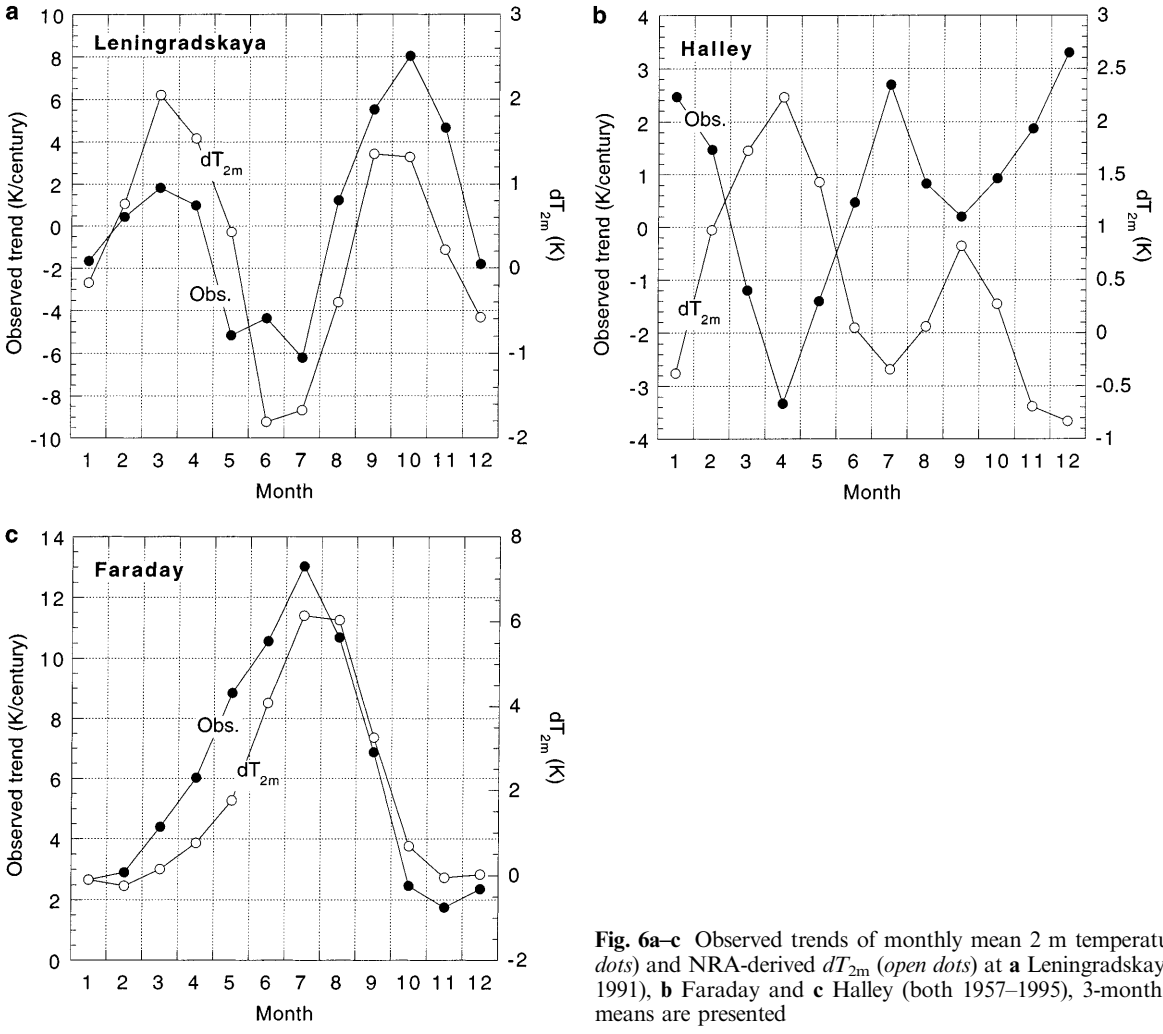

Fig. 6a–c Observed trends of monthly mean 2 m temperature (*solid dots*) and NRA-derived dT_{2m} (*open dots*) at **a** Leningradskaya (1971–1991), **b** Faraday and **c** Halley (both 1957–1995), 3-month running means are presented

den Broeke (2000b) demonstrated that recent changes in wintertime sea-ice cover in the Amundsen/Bellingshausen seas are connected to SAO-decline. This is supported by dT_{2m} in Fig. 6c, which strongly resembles the observed Faraday temperature trends, thus providing further evidence that decadal weakening of the SAO is partly responsible for the strong wintertime warming of the AP region. Analysis of historical radiosonde data must confirm that the warming is largely confined to the atmospheric boundary layer, as the results presented in Sect. 3.2 suggest.

4.3 All stations

In Fig. 7 we compare the composite June/July temperature trends at 11 coastal Antarctic stations with dT_{2m} from NRA (excluding ice shelf stations for reasons mentioned in the previous section). Table 1 lists the stations, June/July temperature trends and data gaps. Note that only the trend at Faraday is significantly different from zero. A weighted correlation yields a slope and intercept of the ordinate that are significant at the 5% level (Fig. 7). The same significance is obtained when a rank correlation is used, that takes into account the obvious non-normal distribution of dT_{2m}. Three station clusters can be detected in Fig. 7:

1. Stations in the sector 60–100°E with small trends and a cooling response to SAO decline (Mawson, Davis, Mirny), obviously caused by increased advection of continental air (Fig. 5a);
2. Stations with slight warming trends but small SAO response, situated in East Antarctica on either side of the first group (Novolazerevskaya, Syowa, Molodezhnaya, Casey, Dumont d'Urville);
3. Stations in the vicinity of the Antarctic Peninsula, with strong warming trends and a warming response to the SAO.

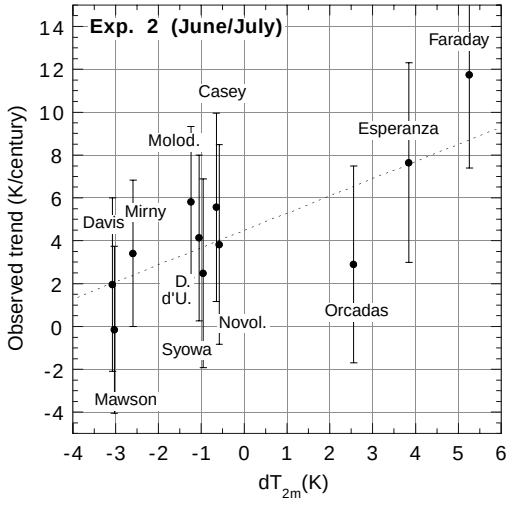

Fig. 7 Composite June/July 2 m temperature trends at 12 coastal Antarctic stations (ice shelf stations excluded) as a function of dT_{2m} (derived from NRA)

Table 1 Combined June/July temperature trend and data gaps for stations used in Fig. 7

Station	June/July T_{2m} trend (K per century)	Years missing (1957–95)
Faraday	11.8 ± 4.4	–
Esperanza	7.7 ± 4.7	1992, 93, 95
Orcadas	2.9 ± 4.6	1975, 95
Novolazerevskaya	3.8 ± 4.7	1957–60, 94
Syowa	2.5 ± 4.4	1958, 62–65
Molodezhnaya	5.8 ± 3.5	1957–62
Mawson	−0.2 ± 3.9	–
Davis	2.0 ± 4.1	1965–68, 80
Mirny	3.4 ± 3.4	–
Casey	5.6 ± 4.4	1957–59
Dumont d'Urville	4.1 ± 3.9	–

The intercept of the ordinate in Fig. 7 is representative of a fictitious station where 2 m temperature is not sensitive to changes in the SAO ($dT_{2m} = 0$). Its value of 4.62 ± 1.02 °C per century is about four times the annual value for Antarctica, as reported by Van den Broeke (J Climate submitted). A stronger wintertime warming is similar to what is found and predicted for the continental polar regions of the Northern Hemisphere (Weller 1998).

5 Discussion

A Significant, long-term weakening of the SAO would be needed to explain the spatial and temporal correlations of dT_{2m} with observed temperature trends. Although a well-documented weakening of the SAO occurred in the late 1970s (Van Loon et al. 1993; Hurrell and Van Loon 1994; Simmonds and Jones 1998), such a trend can not be detected in Fig. 3. However, weaker SAO conditions since 1975 do show up when we look at individual station records. Figure 8 shows time series of the amplitude of $H_2(p)$ at five stations, including the long Orcadas record. To highlight long-term variations, the harmonic analysis was performed on 5-year running means of monthly mean pressure. Comparing the mean

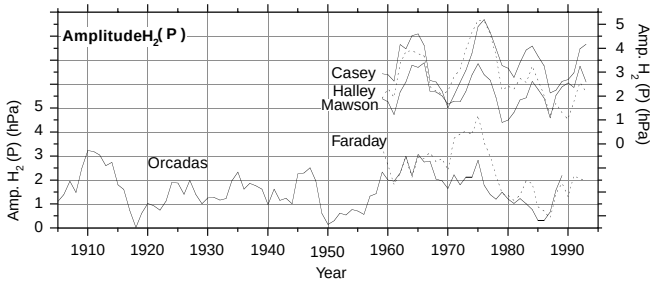

Fig. 8 Time series of the amplitude of $H_2(p)$ at Orcadas and Faraday (*lower pair of lines*, *scale at left axis*) and at Mawson, Halley and Casey (*upper three lines*, *scale at right axis*). To highlight long-term variations, the harmonic analysis was performed on 5-year running means of monthly mean pressure

annual pressure cycle of the period 1980–96 to that prior to 1980, the variance explained by $H_2(p)$ at Faraday has decreased from 77% to less than 10%. Although less dramatic, a decrease is found for all Antarctic stations (Van den Broeke 1998b). From Fig. 8 it appears that this change is part of the natural decadal variability in the SAO, namely the falling branch of a 30–35 year oscillation that is conspicuously present in the Orcadas record, but obscured in the shorter records by a 8–10 year periodicity. If the pattern of the longer Orcadas record proves to be repetitive, the next maximum in SAO activity can be expected in the coming decade. This could prove or falsify the proposed link between the SAO, Antarctic temperature trends and the formation of the Weddell Polynya.

6 Conclusions

Using Antarctic station data and NCEP/NCAR reanalysis we studied the influence of interannual variability of the semiannual oscillation (SAO) on the annual cycle of Antarctic temperature. We found that:

1. In response to changes in the meridional fetch of the circumpolar pressure trough, weak SAO conditions cause Antarctic cooling in the expanded phases (December/January and June/July) and warming in the contracted phases (March/April and September/October). Changes in the expanded phases dominate;
2. The strongest near-surface temperature response is found in *Exp. 2* (June/July), but large regional differences occur: for instance, northwesterly flow anomalies over the Amundsen and Bellingshausen Seas result in decreased sea-ice cover and anomalous strong wintertime warming over the Antarctic Peninsula;
3. Spatial and temporal patterns of observed Antarctic temperature trends strongly resemble those associated with SAO weakening. A background June/July Antarctic warming trend of 4.62 ± 1.02 °C per century can be derived, about four times the annual value;
4. A unique 3 year period of high-amplitude SAO (1974–76) coincided with the formation of the Weddell Polynya. We speculate that this is a result of unfavourable conditions for sea ice growth in the eastern Weddell Sea in *Exp. 2* (June/July);

A period of well-developed SAO in the coming decade could prove of falsify the proposed connections between the SAO, Antarctic temperature trends and the formation of the Weddell Polynya. Important questions that remain are: what causes the decadal variations in the SAO? Are there tropical or global connections? What determines the preferred locations of the climatological lows in the various phases of the SAO? Future work will focus on answering these questions as well as exploring the link between the SAO and the Weddell Polynya and the detection of an SAO signal in Antarctic firn/ice cores.

Acknowledgements We gratefully acknowledge the use of NCEP/NCAR re-analysis data for this work. Additional temperature data were provided by the British Antarctic Survey, the Australian Bureau of Meteorology and Paul Pettré from Météo France. Comments on an earlier version made by William Connolley (British Antarctic Survey) and an anonymous reviewer greatly helped to improve the manuscript.

References

Connolley WM (1997) Variability in annual mean circulation in southern high latitudes. Clim Dyn 13: 745–756
Enomoto H, Ohmura A (1990) The influence of atmospheric half-yearly cycle on the sea ice extent in the Antarctic. J Geophys Res 95 (C6): 9497–9511
Harangozo SA (1997) Atmospheric meridional circulation impacts on contrasting winter sea ice extent in two years in the Pacific sector of the Southern Ocean. Tellus 49A: 388–400
Hurrell JW, van Loon H (1994) A modulation of the atmospheric annual cycle in the Southern Hemisphere. Tellus 46A: 325–338
Jacka TH, Budd WF (1998) Detection of temperature and sea-ice-extent changes in the Antarctic and Southern Ocean, 1949–96. Ann Glacio 27: 553–559
Jacobs SS, Comiso JC (1997) Climate variability in the Amundsen and Bellingshausen Seas. J Clim 10: 697–709
Kalnay E and 21 others (1996) The NCEP/NCAR 40-year reanalysis project. Bull Am Meteorol Soc. 77: 437–471
King JC (1994) Recent climate variability in the vicinity of the Antarctic Peninsula. Int J Climatol 14: 357–369
King JC, Turner J (1997) Antarctic meteorology and climatology. Cambridge University Press, Cambridge, 114, 409 pp
King JC, Harangozo SA (1998) Climate change in the western Antarctic Peninsula since 1945: observations and possible causes. Ann Glaciol 27: 571–575
Marshall GJ, King JC (1998) Southern Hemisphere circulation anomalies associated with extreme Antarctic Peninsula winter temperatures. Geophys Res Lett 25: 2437–2440
Meehl GA (1991) A re-examination of the mechanism of the semi-annual cycle in the Southern Hemisphere. J Clim 4: 911–926
Schwerdtfeger W, Prohaska F (1956) The semiannual pressure oscillation: cause and effects. J Meteorol 13: 217–218
Simmonds I, Walland DJ (1998) Decadal and centennial variability of the southern semiannual oscillation simulated in the GFDL coupled GCM. Clim Dyn 14: 45–53
Simmonds I, Jones DA (1998) The mean structure and temporal variability of the semiannual oscillation in the southern extra-tropics. Int J Climatol 18: 473–504
Turner JS, Colwell R, Harangozo S (1997) Variability of precipitation over coastal western Antarctic Peninsula from synoptic observations. J Geophys Res D12: 13 999–14 007
Van den Broeke MR (1998a) The semiannual oscillation and Antarctic climate, part 1: influence on near-surface temperatures (1957–1979). Antarct Sci 10(2): 175–183
Van den Broeke MR (1998b) The semiannual oscillation and Antarctic climate, part 2: recent changes. Antarct Sci 10(2): 184–191
Van den Broeke MR (2000a) The semiannual oscillation and Antarctic climate, part 3: the role of near-surface wind speed and cloudiness. Int J Climatol (in press)
Van den Broeke MR (2000b) The semiannual oscillation and Antarctic climate, part 4: a note on sea ice cover in the Amundsen and Bellingshausen Seas. Int J Climatol (in press)
Van den Broeke MR, van de Wal RSW, Wild M (1997) Representation of Antarctic katabatic winds in a high resolution GCM and a note on their climate sensitivity. J Clim 10(12): 3111–3130
Van Lipzig NPM (1999) The surface mass balance of the Antarctic ice sheet: a study with a regional atmospheric model, PhD thesis, Utrecht University, 140 pp

Van Loon H (1967) The half-yearly oscillation in the middle and high southern latitudes and the coreless winter. J Atmos Sci 24: 472–486

Van Loon H, Kidson JW, Mullan AB (1993) Decadal variation of the annual cycle in the Australian dataset. J Clim 6: 1227–1231

Vaughan DG, Doake CSM (1996) Recent atmospheric warming and retreat of ice shelves on the Antarctic Peninsula. Nature 379: 328–331

Walland DJ, Simmonds I (1999) Baroclinicity, meridional temperature gradients and the southern semiannual oscillation. J Clim (in press)

Weller G (1998) Regional impacts of climate change in the Arctic and Antarctic. Ann Glaciol 27: 543–552

Wendler G, Kodama Y (1993) The kernlose winter in Adélie coast. In: Bromwich DH, Stearns CR (eds) Antarctic meteorology and climatology, studies based on automatic weather stations. Antarctic Res Ser 61: 139–147